Translational Diffusion Coefficient of Oligo- and Poly(methyl methacrylate)s in Dilute Solutions

Katsuhisa Dehara, Takenao Yoshizaki, and Hiromi Yamakawa*

Department of Polymer Chemistry, Kyoto University, Kyoto 606-01, Japan

*Received May 25, 1993**

ABSTRACT: The translational diffusion coefficient D was determined from dynamic light scattering (DLS) measurements for 14 samples of oligo- and poly(methyl methacrylate)s (a-PMMA), each with the fraction of racemic diads $f_r = 0.79$, in the range of weight-average molecular weight M_w from 5.02×10^2 to 2.18×10^5 in acetonitrile at 44.0 °C (Θ). The determination was also made for the same samples except for the four with the smallest M_w in *n*-butyl chloride at 40.8 °C (Θ). A modification of the DLS data acquisition procedure was made in order to remove the effect of some residual aggregates of solute a-PMMA molecules in acetonitrile. As was expected from the dependence on M_w of the intrinsic viscosity $[\eta]$ reported previously, a double-logarithmic plot of DM_w against M_w in each solvent deviates downward from its asymptotic straight line of slope $1/2$, following an S-shaped curve. A comparison is made of the present results (along with those for two a-PMMA samples with larger M_w reported previously) with the corresponding theory based on the helical wormlike (HW) touched-bead model. The values of the model parameters determined are found to be consistent with those from the previous analyses of $[\eta]$ and the mean-square radius of gyration, confirming that the local and global conformations of the a-PMMA chain in dilute solution may be described typically by the HW chain model.

Introduction

In a series of recent experimental investigations[1-4] on dilute solution properties of atactic oligo- and poly(methyl methacrylate)s (a-PMMA) with the fraction of racemic diads $f_r = 0.79$, we have found that its unperturbed chain in the Θ state shows very salient behavior that cannot be explained on the basis of the Gaussian chain model. Specifically, the ratio of the (unperturbed) mean-square radius of gyration $\langle S^2 \rangle$ to the weight-average molecular weight M_w as a function of M_w exhibits a maximum at $M_w \simeq 5 \times 10^3$,[1] a double-logarithmic plot of the intrinsic viscosity $[\eta]$ against M_w deviates appreciably upward from its asymptotic straight line of slope $1/2$ with decreasing M_w for $M_w \lesssim 6 \times 10^4$, following an inverse S-shaped curve,[2] and the Kratky plot of the scattering function $P(k)$ against the magnitude k of the scattering vector exhibits a (first) maximum followed by a minimum (although no second maximum and minimum).[4] It has then been shown that all these findings characteristic of a-PMMA may well be explained consistently on the basis of the helical wormlike (HW) chain model.[5,6] Thus, in contradiction to the usual notion, the a-PMMA chain has proved to have rather large static stiffness, retaining its large helical portions in dilute solution,[1] compared to other flexible polymers, e.g., atactic polystyrene (a-PS) (with $f_r = 0.59$),[7] polyisobutylene,[8] and poly(dimethylsiloxane) (PDMS).[9] In the present paper, we proceed to make a study of another steady-state transport coefficient, i.e., the translational diffusion coefficient D of the unperturbed a-PMMA chain.

Considering the fact that $[\eta]$ is proportional to the hydrodynamic volume of a single polymer chain in dilute solution, while D is inversely proportional to its hydrodynamic radius, a double-logarithmic plot of DM_w against M_w may be expected to deviate downward from its asymptotic straight line of slope $1/2$ as M_w is decreased, following an S-shaped curve, in accordance with the behavior of $[\eta]$ mentioned above. (Note that the quantity DM_w is proportional to the sedimentation coefficient.) A confirmation of this expectation is one of the purposes of the present work.

In addition to the remarkable behavior of $[\eta]$ mentioned above, it has also been found in the previous study[2] that the values of $[\eta]/M_w^{1/2}$ of a-PMMA samples with sufficiently large M_w in two Θ solvents at their respective Θ temperatures, i.e., acetonitrile at 44.0 °C and *n*-butyl chloride at 40.8 °C, are definitely different from each other, although those of $\langle S^2 \rangle / M_w$ coincide within experimental error. This has led to the conclusion that the coil limiting values Φ_∞ of the Flory-Fox factor for the a-PMMA chain in the two Θ solvents are different from each other.[2] As reported previously for two a-PMMA samples with sufficiently large M_w,[10] the coil limiting values of another transport factor ρ as defined as the ratio of $\langle S^2 \rangle^{1/2}$ to the hydrodynamic radius are also different from each other in these Θ solvents, although the difference is rather small. Thus, from dynamic light scattering (DLS) measurements, we determine D over a wide range of M_w in the same two Θ solvents to compare the results.

It is pertinent to make here a remark on the experimental determination of the (normalized) autocorrelation function of scattered light intensity $g^{(2)}(t)$ as a function of time t for acetonitrile solutions of a-PMMA. For dilute polymer solutions, a plot of $\ln[g^{(2)}(t) - 1]$ against t at sufficiently small scattering angles in general follows a straight line for such large t that all the internal motions of solute polymer chains have relaxed away. However, the plot for the acetonitrile solutions of a-PMMA samples with low M_w was found to follow a curve concave upward without reproducibility, indicating that there were some unidentified particles with small mobility in test solutions. At first, considering that it arose from an incomplete optical purification of test solutions, we repeated the purification. Unfortunately, however, the above anomalous behavior could not be suppressed. Thus we have concluded that the unidentified particles are not dust but some residual aggregates of solute a-PMMA molecules and decided to remove their effect by modifying our data acquisition procedure. It may then be possible to determine D for dispersed a-PMMA molecules from the data for $g^{(2)}(t)$ affected by the aggregates by an application of, for instance, the CONTIN analysis,[11] but we have devised a direct method which may be regarded as more accurate for the present problem.

* Abstract published in *Advance ACS Abstracts,* August 15, 1993.

0024-9297/93/2226-5137$04.00/0

Table I. Values of M_w, x_w, and M_w/M_n for Atactic Oligo- and Poly(methyl methacrylate)s

sample	M_w	x_w	M_w/M_n
OM5	5.02×10^2	5	1.00
OM6	6.02×10^2	6.00	1.00
OM8	7.98×10^2	7.96	1.00
OM12[a]	1.16×10^3	11.6	1.02
OM18	1.80×10^3	18.0	1.07
OM30	2.95×10^3	29.5	1.06
OM42	4.18×10^3	41.8	1.09
OM76	7.55×10^3	75.5	1.08
MM1[b]	1.09×10^4	109	1.06
MM2a	2.02×10^4	202	1.08
MM4	3.53×10^4	353	1.07
MM7	7.40×10^4	740	1.09
MM12	1.19×10^5	1190	1.09
MM22	2.18×10^5	2180	1.06

[a] M_w's of OM12 through OM76 and MM2a had been determined from LS measurements in acetone at 25.0 °C.[1,12] [b] M_w's of MM1 through MM22 except for MM2a had been determined from LS measurements in acetonitrile at 44.0 °C.[1]

Experimental Section

Materials. Most of the a-PMMA samples used in this work are the same as those used in the previous studies,[1,2] i.e., the fractions separated by gel permeation chromatography (GPC) or fractional precipitation from the original samples prepared by group-transfer polymerization (GTP). In the course of repeated measurements carried out in the previous studies,[1-4] especially in that of the mean-square optical anisotropy $\langle\Gamma^2\rangle$,[3] some of the samples prepared previously[1] had been wasted and their remainders had not been ample for this work. Thus some additional samples were prepared in the same manner as before,[1] i.e., by GTP, followed by separation by GPC or fractional precipitation. The values of the fraction of racemic diads f_r for them were examined by ^{13}C NMR in the same manner as before[1] and were found to coincide with the previous value 0.79 independent of M_w.

The values of M_w obtained from analytical GPC ($M_w < 10^3$) and light scattering (LS) measurements ($M_w > 10^3$) are given in Table I along with those of the weight-average degree of polymerization x_w and the ratio of M_w to the number-average molecular weight M_n. The samples OM12, OM42, OM76, and MM2a are the additional ones, and their M_w's were determined from LS measurements in acetone at 25.0 °C. The details will be given elsewhere.[12] The sample OM5 is also an additional one, which can be completely identified with the previous one since both of them are monodisperse with the same f_r.

The solvents acetonitrile and *n*-butyl chloride used for DLS measurements were purified according to standard procedures.

Dynamic Light Scattering. (i) Measurements. DLS measurements were carried out to determine D for the 14 a-PMMA samples in acetonitrile at 44.0 °C (Θ) and in *n*-butyl chloride at 40.8 °C (Θ) by the use of a Brookhaven Instruments Model BI-200SM light scattering goniometer with vertically polarized incident light of 488-nm wavelength from a Spectra-Physics Model 2020 argon ion laser equipped with a Model 583 temperature-stabilized etalon for single-frequency-mode operation. The photomultiplier tube used was EMI 9893B/350, the output from which was processed by a Brookhaven Instruments Model BI2030AT autocorrelator with 264 channels. A minor modification has been made of the detector alignment as described before.[10] The normalized autocorrelation function $g^{(2)}(t)$ of scattered light intensity $I(t)$ at time t was measured at four or five concentrations for almost all cases and at scattering angles θ ranging from 20 to 110°.

The most concentrated solutions of the samples in the two solvents were prepared by continuous stirring for 1 day at ca. 50 °C. These solutions were optically purified by filtration through a Teflon membrane of 0.1- or 0.45-μm pore size. All the solutions of lower concentrations were obtained by dilution. We note that a special care required in the preparation of *n*-butyl chloride solutions[2] is not necessary for the samples with $M_w < 3 \times 10^5$. The weight concentrations of test solutions were determined gravimetrically and converted to the mass concentrations c by the use of the densities of the solutions.

(ii) Data Acquisition. From the data for $g^{(2)}(t)$ measured at finite concentrations c, we determine the translational diffusion coefficient *at an infinitely long time*[13] at infinite dilution in the same manner as that used in previous studies.[10,13,14] At small c, a plot of $(1/2)\ln[g^{(2)}(t) - 1]$ against t in general follows a straight line,

$$(1/2)\ln[g^{(2)}(t) - 1] = \text{const} - At \tag{1}$$

with A the slope for such large t that all the internal motions of solute polymer chains have relaxed away.[13]

As mentioned in the Introduction, however, for acetonitrile solutions of a-PMMA samples with small M_w the plot was found to follow a curve concave upward without reproducibility. This may be regarded as arising from some residual aggregates of solute a-PMMA molecules, and their effect was found to become remarkable for the samples with small M_w. The reason for this is that the intensity of the light scattered by solute molecules decreases with decreasing M_w, so that for small M_w we must use test solutions of such high concentrations that the aggregates may be produced. We note that these aggregates, whose amount is small, affect the shape of the plot at rather large t but not at $t \simeq 0$ and therefore have no effect on the static LS, in which case the average intensity, i.e., the square root of (unnormalized) $g^{(2)}(0)$, is measured. This effect may be removed by the use of the following data acquisition procedure.

In the DLS measurement using our apparatus, we obtain data for the primitive quantity $C_n(j\tau)$ (j = 1, 2, ..., 264, 1291, 1292, ..., 1296) defined by

$$C_n(j\tau) = \sum_{p=1}^{n} N(p)\, N(p+j) \tag{2}$$

where τ is the sampling time and $N(p)$ is the number of photons counted at the pth time interval. Note that the number $N(p)$ is proportional to the mean intensity $\bar{I}(p\tau)$ of the scattered light averaged over the pth interval,

$$N(p) \propto \bar{I}(p\tau) \equiv \frac{1}{\tau}\int_{(p-1/2)\tau}^{(p+1/2)\tau} I(t)\, dt \tag{3}$$

where we have omitted the "dead time", i.e., a pause placed between two successive intervals. The upper bound n of the summation over p on the right-hand side of eq 2 is actually taken to be so large ($\gtrsim 10^8$) that eq 2 may be rewritten as

$$C_n(j\tau) = n\langle N(0)\, N(j)\rangle \tag{4}$$

In addition to the above set of 264 + 6 values of $C_n(j\tau)$, we obtain the quantities B_{calc} and B_{obs} defined by

$$B_{calc} \equiv C_n(\infty) = n\langle N(0)\rangle^2 \tag{5}$$

and

$$B_{obs} \equiv \frac{1}{6}\sum_{j=1291}^{1296} C_n(j\tau) \tag{6}$$

respectively. Note that the value of B_{obs} must become identical with that of B_{calc} if the times $j\tau$ (j = 1291, 1292, ..., 1296) are sufficiently large compared to the relaxation time characteristic of the system under consideration. The quantity $g^{(2)}(t)$ may then be written in terms of $C_n(j\tau)$ and B_{calc} as

$$g^{(2)}(t) = \langle\bar{I}(0)\,\bar{I}(j\tau)\rangle/\langle\bar{I}(0)\rangle^2 = C_n(j\tau)/B_{calc} \tag{7}$$

where

$$t = j\tau \tag{8}$$

In the usual measurements, the data accumulation is made to a proper extent, assigning a proper value to the upper bound n of the summation on the right-hand side of eq 2 so that the statistical error may be suppressed within the range of allowance. If a few aggregates cross the scattering volume during the time $n\tau$, then B_{obs} becomes somewhat larger than B_{calc} since the relaxation time of the intensity fluctuation caused by them is extraordinarily large compared to that for dispersed a-PMMA

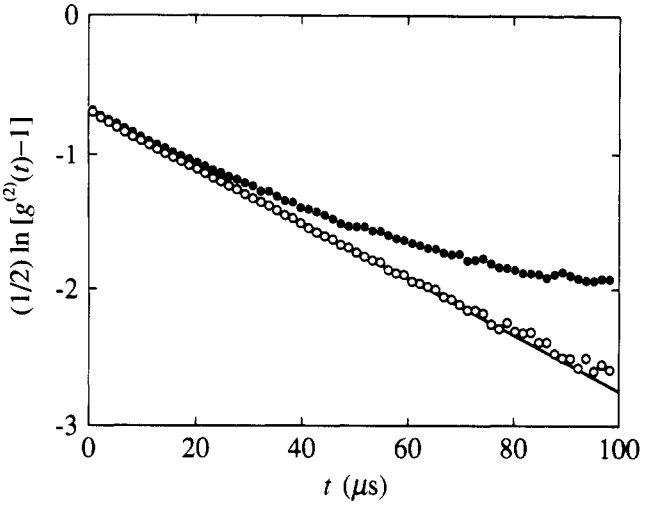

Figure 1. Plots of $(1/2)\ln[g^{(2)}(t)-1]$ against t for the a-PMMA sample OM30 in acetonitrile at 44.0 °C, at $c = 4.28 \times 10^{-2}$ g/cm^3, and at $\theta = 20°$: (○) data by the new procedure; (●) data by the usual procedure.

molecules and thus the plot of $(1/2)\ln[g^{(2)}(t)-1]$ against t becomes concave upward. The maneuver we adopt for the elimination of this effect is very simple; i.e., we replace a single measurement during the time $n\tau$ by a set of many measurements, each being made during the time $m\tau$ ($n \gg m \gg 1$), and discard those results which have been affected by the aggregates. Then C_n may be written in the form

$$C_n(j\tau) = \sum_{l=1}^{l_{max}} f(B_{obs}^{(l)}/B_{calc}^{(l)} - 1 - \delta)\, C_m^{(l)}(j\tau) \tag{9}$$

where $f(x) = 1 - h(x)$ with $h(x)$ being a unit step function such that $h(x) = 1$ for $x \geq 0$ and $h(x) = 0$ for $x < 0$, δ is the threshold value properly chosen, and $C_m^{(l)}(j\tau)$ is the result of the lth measurement during the time $m\tau$. The upper bound l_{max} of the summation over l is chosen in such a way that the resultant effective measurement time may be identical with $n\tau$, i.e.,

$$\sum_{l=1}^{l_{max}} f(B_{obs}^{(l)}/B_{calc}^{(l)} - 1 - \delta) = n/m \tag{10}$$

Then $g^{(2)}(t)$ may be given by eq 7 with eq 9. In practice, $m\tau$ and δ were taken as 20 s and 0.01, respectively.

Figure 1 shows plots of $(1/2)\ln[g^{(2)}(t) - 1]$ against t for the sample OM30 in acetonitrile at 44.0 °C, at $c = 4.28 \times 10^{-2}$ g/cm^3, and at $\theta = 20°$. In this case, the sampling time and the whole effective measurement time are 1 μs and 600 s, respectively. The unfilled and filled circles represent the data obtained by the new procedure based on eq 7 with eq 9 and by the usual procedure based on eq 7 with eq 2, respectively. It is clearly seen that the new procedure is so effective that the slope of the plot may be determined with sufficient accuracy.

Now, with the slope A thus evaluated, we may determine the apparent diffusion coefficient $D^{(LS)}(c)$ at finite c from

$$D^{(LS)}(c) = \lim_{k \to 0} A/k^2 \tag{11}$$

where k is the magnitude of the scattering vector and is given by

$$k = (4\pi/\tilde{\lambda}) \sin(\theta/2) \tag{12}$$

with $\tilde{\lambda}$ the wavelength of the incident light in the solvent. At sufficiently low c, $D^{(LS)}(c)$ may be expanded as

$$D^{(LS)}(c) = D^{(LS)}(0)\,(1 + k_D^{(LS)} c + \ldots) \tag{13}$$

so that $D = D(\infty)$ (at an infinitely long time) may be determined from extrapolation of $D^{(LS)}(c)$ to $c = 0$ as

$$D = D^{(LS)}(0) \tag{14}$$

We note that the slope A can be determined by the usual procedure in the case of the n-butyl chloride solutions.

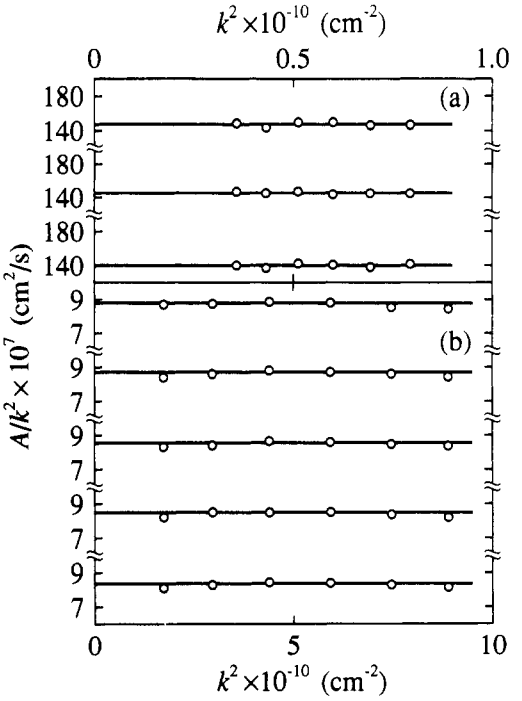

Figure 2. Plots of A/k^2 against k^2 for the a-PMMA samples OM5 (a) and MM22 (b) in acetonitrile at 44.0 °C. The polymer mass concentrations c are 9.17×10^{-2}, 1.11×10^{-1}, and 1.39×10^{-1} g/cm^3 for case a and 5.55×10^{-4}, 8.82×10^{-4}, 1.34×10^{-3}, 1.79×10^{-3}, and 2.32×10^{-5} g/cm^3 for case b from top to bottom.

The values of the refractive index we used at a wavelength of 488 nm are 1.337 in acetonitrile at 44.0 °C and 1.397 in n-butyl chloride at 40.8 °C. The values of the viscosity coefficient η_0 we used for them are 0.285 and 0.362 cP, respectively.

Results

Figure 2 shows plots of A/k^2 against k^2 for the samples OM5 (a) and MM22 (b) in acetonitrile at 44.0 °C, the data points representing the values at $c = 9.17 \times 10^{-2}$, 1.11×10^{-1}, and 1.39×10^{-1} g/cm^3 for OM5 and at $c = 5.55 \times 10^{-4}$, 8.82×10^{-4}, 1.34×10^{-3}, 1.79×10^{-3}, and 2.32×10^{-3} g/cm^3 for MM22 from top to bottom. In the range of k^2 displayed, A/k^2 is almost independent of k^2, so that we adopt as the value of $D^{(LS)}(c)$ $[=(A/k^2)_{k=0}]$ at each finite c the mean value represented by the horizontal line. For the other samples in acetonitrile, $D^{(LS)}(c)$ could be determined in the same way. As for n-butyl chloride solutions, $D^{(LS)}(c)$ for the samples with $M_w \gtrsim 1.5 \times 10^3$, i.e., the samples OM18 through MM22, could also be determined rather accurately (by the usual procedure). Unfortunately, however, $D^{(LS)}(c)$ could not be determined for the samples OM5 through OM12 with sufficient accuracy, since the values of the refractive index increment $\partial n/\partial c$ for n-butyl chloride solutions of a-PMMA at 40.8 °C are rather small (e.g., 0.099 cm^3/g for the samples[2] with sufficiently large M_w) compared to that for the acetonitrile solutions at 44.0 °C (e.g., 0.144 cm^3/g for the samples[1] with sufficiently large M_w). Note that $\partial n/\partial c$ decreases with decreasing M_w for $M_w \lesssim 10^4$ for both solutions.

Figure 3 shows plots of the values of $D^{(LS)}(c)$ thus determined against c for the 14 a-PMMA samples indicated in acetonitrile at 44.0 °C. Figure 4 shows similar plots for the 10 samples except for the four samples OM5 through OM12 in n-butyl chloride at 40.8 °C. As seen from these figures, the data points for each system follow a straight line, and therefore $D(0)$ $(=D)$ and $k_D^{(LS)}$ may be determined from the ordinate intercept and slope, respectively. In Table II are given the values of D and $k_D^{(LS)}$ thus

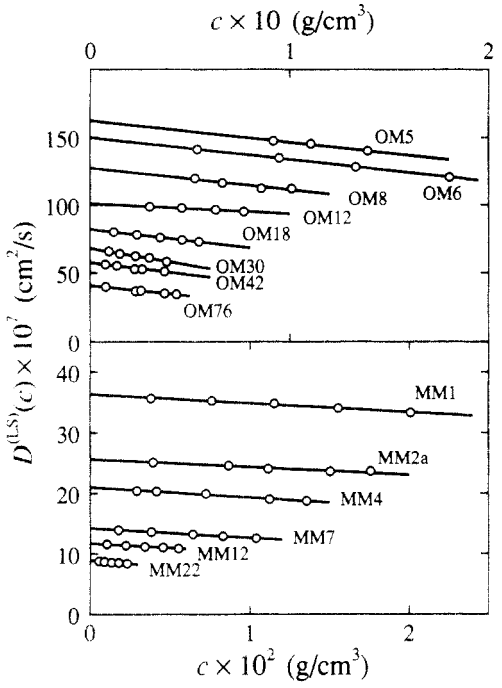

Figure 3. Plots of $D^{(LS)}(c)$ against c for the a-PMMA samples indicated in acetonitrile at 44.0 °C.

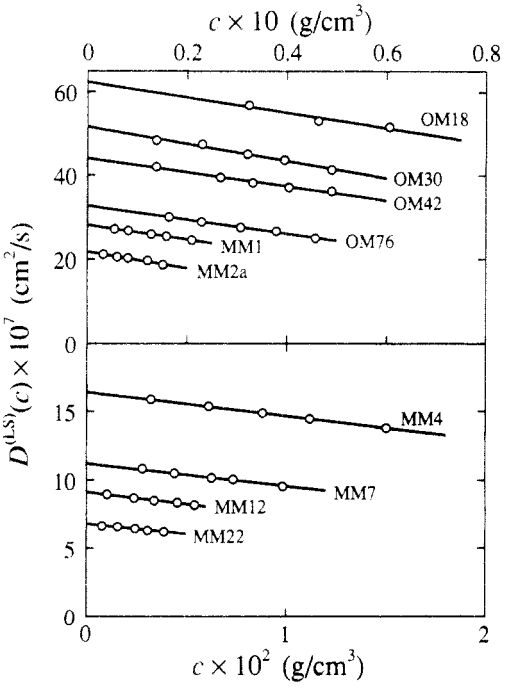

Figure 4. Plots of $D^{(LS)}(c)$ against c for the a-PMMA samples indicated in n-butyl chloride at 40.8 °C.

obtained along with those for the two a-PMMA samples Mr4 with $M_w = 3.61 \times 10^5$ and Mr8 with $M_w = 7.58 \times 10^5$ determined previously[10] (although the values of $k_D^{(LS)}$ had not been reported). Note that the values of M_w for these two samples are those determined from LS measurements in acetonitrile at 44.0 °C.[1]

Figure 5 shows double-logarithmic plots of $\eta_0 DM_w/k_BT$ (in cm^{-1}) against M_w with the data in acetonitrile at 44.0 °C (unfilled circles) and in n-butyl chloride at 40.8 °C (filled circles), where k_B is the Boltzmann constant and T is the absolute temperature. The solid curves connect the respective data points smoothly, and the dotted lines indicate their respective asymptotic straight lines of slope $1/2$. For both solutions, the data points deviate downward from their asymptotic straight lines for $M_w \lesssim 5 \times 10^4$, each

Table II. Results of DLS Measurements on Atactic Oligo- and Poly(methyl methacrylate)s in Acetonitrile at 44.0 °C and in n-Butyl Chloride at 40.8 °C

	acetonitrile (44.0 °C)		n-butyl chloride (40.8 °C)	
sample	10^7D, cm^2/s	$k_D^{(LS)}$, cm^3/g	10^7D, cm^2/s	$k_D^{(LS)}$, cm^3/g
OM5	163	−1.0		
OM6	150	−1.1		
OM8	128	−1.3		
OM12	101	−0.7		
OM18	82.1	−2.1	62.4	−3.0
OM30	68.0	−3.7	51.5	−4.0
OM42	57.5	−3.1	44.0	−3.8
OM76	40.8	−3.7	32.7	−5.1
MM1	36.4	−4.1	28.1	−6.1
MM2a	25.6	−5.1	21.8	−9.0
MM4	21.0	−8.1	16.4	−10.7
MM7	14.3	−11.4	11.2	−14.6
MM12	11.6	−13.2	9.13	−18.8
MM22	8.89	−24.2	6.82	−22.4
Mr4[a]	6.84	−29.2	5.25	−28.6
Mr8	4.73	−57.1	3.58	−46.1

[a] The values of D of Mr4 and Mr8 in the two solvents have been reproduced from ref 10.

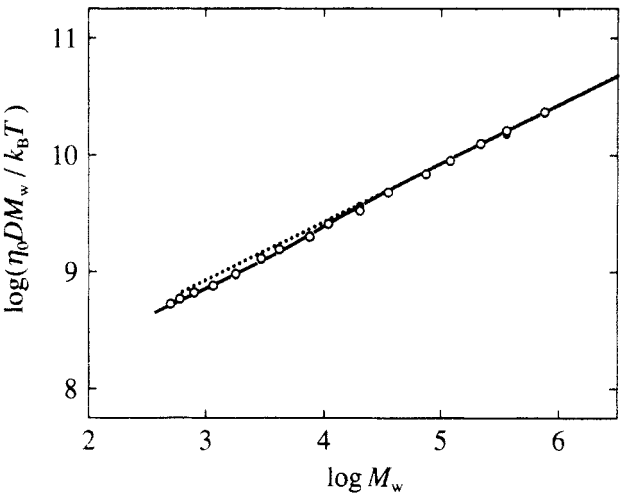

Figure 5. Double-logarithmic plots of $\eta_0 DM_w/k_BT$ (in cm^{-1}) against M_w for a-PMMA: (○) in acetonitrile at 44.0 °C; (●) in n-butyl chloride at 40.8 °C. The dotted straight line has a slope of $1/2$.

set of data following an S-shaped curve, as was expected. It is also interesting to note that the values of $\eta_0 D/T$ in acetonitrile are ca. 3% larger than those in n-butyl chloride for $M_w \gtrsim 2 \times 10^5$, but the two sets of data become identical with each other for smaller M_w within experimental error. Recall that the values of $[\eta]$ in n-butyl chloride are (more than 7%) larger than those in acetonitrile over the whole range of M_w examined.[2] However, we note that the error is larger in D than in $[\eta]$, especially for small M_w ($\lesssim 10^4$).

Discussion

HW Model Parameters. The HW chain[6,7] may be described in terms of the four basic model parameters: the differential-geometrical curvature κ_0 and torsion τ_0 of its characteristic helix taken at the minimum zero of its elastic energy, the static stiffness parameter λ^{-1}, and the shift factor M_L as defined as the molecular weight per unit contour length. Now, for the HW touched-bead model with the total number N of beads or of the total contour length $L = Nd_b$ with d_b the diameter of the bead, the quantity $\eta_0 DM_w/k_BT$ may be written in the form[14]

$$\eta_0 DM_w/k_BT = (M_L/3\pi) f_D(\lambda L;\lambda^{-1}\kappa_0,\lambda^{-1}\tau_0,\lambda d_b) \quad (15)$$

where the function f_D is given by eq 6 of ref 14 and may

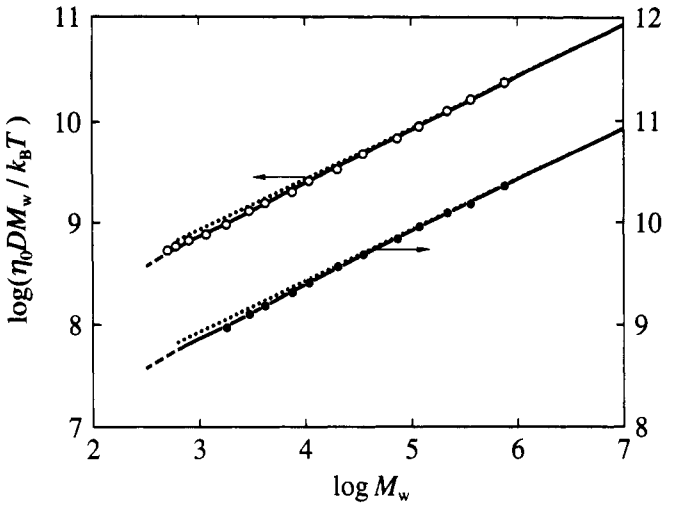

Figure 6. Double-logarithmic plots of $\eta_0 DM_w/k_BT$ (in cm^{-1}) against M_w for a-PMMA: (○) in acetonitrile at 44.0 °C; (●) in *n*-butyl chloride at 40.8 °C. The solid curves represent the best-fit HW theoretical values for $N \geq 2$, with the dashed line segments connecting the respective values for $N = 1$ and 2. The dotted straight lines have a slope of $^1/_2$.

be evaluated by the use of the interpolation formula for the mean reciprocal end-to-end distance of the chain as given in the appendix of ref 15. The function f_D satisfies the asymptotic relation

$$\lim_{\lambda L \to \infty} f_D(\lambda L)/(\lambda L)^{1/2} = (\sqrt{6}/2)c_\infty^{1/2}\rho_\infty \qquad (16)$$

with

$$c_\infty = \frac{4 + (\lambda^{-1}\tau_0)^2}{4 + (\lambda^{-1}\kappa_0)^2 + (\lambda^{-1}\tau_0)^2} \qquad (17)$$

and with ρ_∞(=1.505) being the coil limiting value of the ratio ρ of $\langle S^2\rangle^{1/2}$ to the hydrodynamic radius $R_H = k_BT/6\pi\eta_0 D$.

The basic equation for an analysis of the data for D is given, from eq 15, by

$$\log(\eta_0 DM_w/k_BT) = \log f_D(\lambda L) + \log M_L - 0.975 \qquad (18)$$

along with

$$\log M_w = \log(\lambda L) + \log(\lambda^{-1}M_L) \qquad (19)$$

The quantities M_L and $\lambda^{-1}M_L$ (and therefore λ^{-1} and M_L) may be estimated from a best fit of double-logarithmic plots of the theoretical f_D against λL for properly chosen values of $\lambda^{-1}\kappa_0$, $\lambda^{-1}\tau_0$, and λd_b to that of the observed $\eta_0 DM_w/k_BT$ against M_w, so that we may in principle determine the five parameters $\lambda^{-1}\kappa_0$, $\lambda^{-1}\tau_0$, λ^{-1}, M_L, and d_b. However, in the present analysis, for simplicity, we assume that $\lambda^{-1}\kappa_0$ and $\lambda^{-1}\tau_0$ are the same as those estimated previously[2] from the analysis of the data for $[\eta]$ in acetonitrile at 44.0 °C and in *n*-butyl chloride at 40.8 °C and determine the remaining three parameters λ^{-1}, M_L, and d_b. Further, we ignore the small difference between the data for $\eta_0 D/T$ in the two solvents.

Figure 6 shows double-logarithmic plots of $\eta_0 DM_w/k_BT$ against M_w for a-PMMA in acetonitrile at 44.0 °C (unfilled circles) and in *n*-butyl chloride at 40.8 °C (filled circles). The solid curve associated with the data points in acetonitrile represents the best-fit theoretical values calculated from eqs 18 and 19 with eq 15 with $\lambda^{-1}\kappa_0 = 4.5$, $\lambda^{-1}\tau_0 = 2.0$, $\lambda d_b = 0.14$, $\log M_L = 1.544$, and $\log \lambda^{-1}M_L = 3.370$, with the dashed line segment connecting those values for $N = 1$ and 2. The solid curve for the data points in *n*-butyl chloride is just the same as the above curve for the data points in acetonitrile. The dotted lines indicate the respective asymptotic straight lines of slope $^1/_2$. It is seen that the agreement between theory and experiment is very good.

Table III. Values of the HW Model Parameters for Atactic Poly(methyl methacrylate) with f_r = 0.79 in Acetonitrile at 44.0 °C

$\lambda^{-1}\kappa_0$	$\lambda^{-1}\tau_0$	λ^{-1}, Å	M_L, Å^{-1}	d_b, Å	obsd quantity
(4.5)	(2.0)	65.0	35.0	9.0	D
4.5	2.0	45.0	38.6	7.2	$[\eta]^a$
4.0	1.1	57.9	36.3		$\langle S^2\rangle^b$

[a] See ref 2. [b] See ref 1.

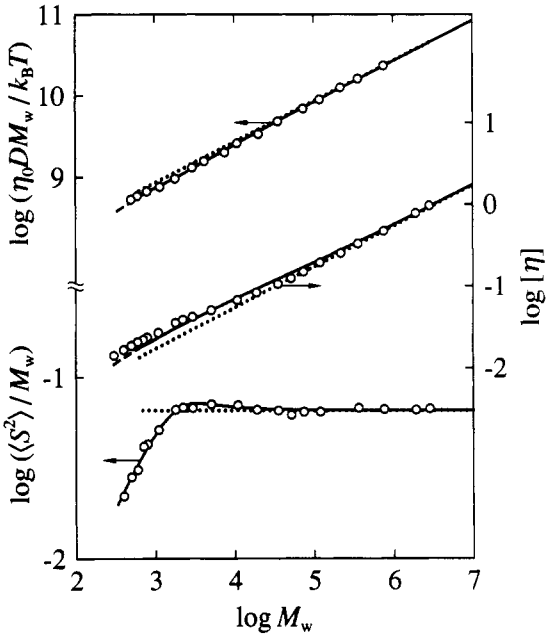

Figure 7. Double-logarithmic plots of $\eta_0 DM_w/k_BT$ (in cm^{-1}), $[\eta]$ (in dL/g),[2] and $\langle S^2\rangle/M_w$ (in Å^2)[1] against M_w for a-PMMA in acetonitrile at 44.0 °C. The solid curves represent the respective best-fit HW theoretical values, with the dashed line segments for the upper two plots connecting the respective values for $N = 1$ and 2. The dotted straight lines have a slope of $^1/_2$ for the upper two and of 0 for the lowest.

The values of the HW model parameters thus determined are listed in the first row of Table III. There are also given the values determined previously[1,2] from the analyses of $[\eta]$ and $\langle S^2\rangle$ in acetonitrile at 44.0 °C. The value 65.0 Å of λ^{-1} determined from D is somewhat larger than that determined from $[\eta]$, while the value 35.0 Å^{-1} of M_L determined from the former is somewhat smaller than that determined from the latter. This tendency is the same as in the cases of a-PS[14] and PDMS[13] and may be regarded as arising from the disagreement between the theoretical and experimental values of the transport factors ρ and Φ in the random-coil limit.[10]

Comparison with $[\eta]$ and $\langle S^2\rangle$. In Figure 7, the data for the three quantities $\eta_0 DM_w/k_BT$ (in cm^{-1}), $[\eta]$ (in dL/g),[2] and $\langle S^2\rangle/M_w$ (in Å^2)[1] for a-PMMA in acetonitrile at 44.0 °C are double-logarithmically plotted against M_w simultaneously. The solid curves represent the respective best-fit HW theoretical values calculated with the values of the model parameters given in Table III. The dashed line segments for the cases of $\eta_0 DM_w/k_BT$ and $[\eta]$ again connect the respective theoretical values for $N = 1$ and 2. The dotted lines for $\eta_0 DM_w/k_BT$ and $[\eta]$ indicate the respective asymptotic straight lines of slope $^1/_2$, and that for $\langle S^2\rangle/M_w$ indicates the asymptotic straight line of slope 0. We note that, although the ratio $\langle S^2\rangle/x_w$ instead of

$\langle S^2\rangle/M_w$ was considered in the previous study,[1] the dependence of the former on x_w is almost equivalent to that of $\langle S^2\rangle/M_w$ on M_w since the ratio M_w/x_w is almost independent of M_w over the whole range of M_w examined, including the oligomer region. The theory may well explain all the experimental data consistently except for $[\eta]$ in the intermediate region.

It is seen that the data for D and $[\eta]$ deviate from the respective asymptotic straight lines at rather large (and almost the same) M_w ($\simeq 5 \times 10^4$), while those for $\langle S^2\rangle$ deviate at somewhat smaller M_w ($\simeq 10^4$), all these S-shaped or inverse S-shaped deviations reflecting strongly the local conformation characteristic of the a-PMMA chain as mentioned in the Introduction. The results are in contrast to the case of a-PS,[14,16-18] for which, for instance, the Houwink–Mark–Sakurada relation holds over a wider range of M_w, while $\langle S^2\rangle$ reaches its Gaussian value at larger M_w ($\simeq 10^5$).

Conclusion

We have been able to determine rather accurately the translational diffusion coefficient D for the oligomer and polymer samples of a-PMMA in acetonitrile at 44.0 °C (Θ) by modifying our DLS data acquisition procedure despite the fact that some residual aggregates of the solute molecules remain unresolved in the case of small M_w. For the *n*-butyl chloride solutions at 40.8 °C (Θ), D has been determined by the usual procedure for the same a-PMMA samples except for the four with the smallest M_w, whose refractive index increments in this solvent are so small that their D cannot be determined with sufficient accuracy.

As was expected from the dependence of $[\eta]$ on M_w, a double-logarithmic plot of $\eta_0 D M_w/k_B T$ against M_w has been found to deviate downward from its asymptotic straight line of slope $^1/_2$ with decreasing M_w, following an S-shaped curve. Although the values of $\eta_0 D M_w/k_B T$ in acetonitrile are somewhat (ca. 3%) larger than those in *n*-butyl chloride for the three samples with the largest M_w, the values for the other samples in the two solvents agree with each other within experimental error. This is in contrast to the previous result that the values of $[\eta]$ in *n*-butyl chloride are definitely larger than those in acetonitrile over the whole range of M_w examined.[2] (However, note that the error is larger in D.) The above salient experimental results can be explained quantitatively by the HW theory with the values of the model parameters consistent with those determined from the previous analyses[1,2] of $\langle S^2\rangle$ and $[\eta]$, confirming that the local and global conformations of the a-PMMA chain in dilute solution may be described typically by the HW chain model. Thus this is our final experimental study of the equilibrium conformational and steady-state transport properties of a-PMMA in the unperturbed Θ state. In forthcoming papers, we proceed to make a similar study of isotactic oligo- and poly(methyl methacrylate)s in order to examine the dependence of the above properties on the stereochemical composition f_r of the chain.

Acknowledgment. This research was supported in part by a Grant-in-Aid (0143 0018) from the Ministry of Education, Science, and Culture, Japan.

References and Notes

(1) Tamai, Y.; Konishi, T.; Einaga, Y.; Fujii, M.; Yamakawa, H. *Macromolecules* **1990**, *23*, 4067.
(2) Fujii, Y.; Tamai, Y.; Konishi, T.; Yamakawa, H. *Macromolecules* **1991**, *24*, 1608.
(3) Takaeda, Y.; Yoshizaki, T.; Yamakawa, H. *Macromolecules* **1993**, *26*, 3742.
(4) Yoshizaki, T.; Hayashi, H.; Yamakawa, H. *Macromolecules* **1993**, *26*, 4037.
(5) Yamakawa, H. *Annu. Rev. Phys. Chem.* **1984**, *35*, 23.
(6) Yamakawa. H. In *Molecular Conformation and Dynamics of Macromolecules in Condensed Systems*; Nagasawa, M., Ed.; Elsevier: Amsterdam, 1988; p 21.
(7) Konishi, T.; Yoshizaki, T.; Shimada, J.; Yamakawa, H. *Macromolecules* **1989**, *22*, 1921 and succeeding papers.
(8) Abe, F.; Einaga, Y.; Yamakawa, H. *Macromolecules* **1991**, *24*, 4423.
(9) Yamada, T.; Yoshizaki, T.; Yamakawa, H. *Macromolecules* **1992**, *25*, 1487 and succeeding paper.
(10) Konishi, T.; Yoshizaki, T.; Yamakawa, H. *Macromolecules* **1991**, *24*, 5614.
(11) Provencher, S. W. *Makromol. Chem.* **1979**, *180*, 201.
(12) Abe, F.; Horita, K.; Einaga, Y.; Yamakawa, H. *Macromolecules*, to be submitted for publication.
(13) Yamada, T.; Koyama, H.; Yoshizaki, T.; Einaga, Y.; Yamakawa, H. *Macromolecules* **1993**, *26*, 2566.
(14) Yamada, T.; Yoshizaki, T.; Yamakawa, H. *Macromolecules* **1992**, *25*, 377.
(15) Yamakawa, H.; Yoshizaki, T. *J. Chem. Phys.* **1983**, *78*, 572.
(16) Einaga, Y.; Koyama, H.; Konishi, T.; Yamakawa, H. *Macromolecules* **1989**, *22*, 3419.
(17) Konishi, T.; Yoshizaki, T.; Saito, T.; Einaga, Y.; Yamakawa, H. *Macromolecules* **1990**, *23*, 290.
(18) Horita, K.; Abe, F.; Einaga, Y.; Yamakawa, H. *Macromolecules*, in press.